Renewable Energy 147 (2020) 2774–2790

Contents lists available at ScienceDirect

Renewable Energy

journal homepage: www.elsevier.com/locate/renene

Investigation of a hybrid system with ground source heat pump and solar collectors: Charging of thermal storages and space heating

Aleksandar Georgiev [a, *], Rumen Popov [b], Emil Toshkov [a]

[a] Department of Mechanics, Faculty of Mechanical Engineering, Technical University of Sofia, Plovdiv Branch, Plovdiv, 4000, Bulgaria
[b] EKIT Department, Faculty of Physics and Technology, Plovdiv University "Paisii Hilendarski", Plovdiv, 4000, Bulgaria

ARTICLE INFO

Article history:
Received 19 June 2018
Received in revised form
19 December 2018
Accepted 24 December 2018
Available online 29 December 2018

Keywords:
Hybrid thermal system
Solar collectors (SC)
Borehole heat exchanger (BHE)
Thermal energy charging
Ground source heat pump heating (GSHPH)
Solar assisted heat pump heating (SAHPH)

ABSTRACT

A hybrid installation that includes solar collectors and a ground source heat pump was developed and tested. There are many studies in the field of combined heat pump systems describing relatively large installations, designed for climatic conditions and soil thermal properties different from those in Bulgaria, where the experimental data are limited. The paper presents the construction of a small size hybrid installation containing diurnal and seasonal storages and supporting five different modes of operation with emphasis on the charging of borehole heat exchanger (BHE), heating mode with ground source heat pump (GSHP) and the followed natural relaxation. The paper also proposes a methodology for determination of different system energy efficiencies. High quality data for the different system operation modes in terms of soil and weather conditions typical of the Plovdiv region were obtained.

The study proves the necessity of BHE charging with thermal energy from the sun during the summer mainly to avoid the ground thermal depletion. The comparison of the three heating modes investigated shows evident advantage of the ground source heat pump heating (GSHPH). The installation must be tested in the future for a longer time period.

© 2018 Elsevier Ltd. All rights reserved.

1. Introduction

The usage of the ground as an energy source for the ground source heat pumps has been well established, but the exploitation for long periods leads to annual imbalances in the ground loads [1]. To overcome this problem, hybrid systems can be used, combining solar collectors as an additional source of energy, which is injected into the ground. Heat injection into the ground by means of solar collectors is presented in several articles [1–3]. Some authors show that the stored energy in the ground during the summer ensures a stable source of heat in the winter time [4–6]. Another alternative is to increase the length of the vertical borehole heat exchangers (BHE), but the drilling costs are still significant. An interesting idea is presented in Ref. [4], where a double loop is used in the same borehole to inject simultaneously solar energy and extract geothermal heat in winter. A detailed experimental investigation of a solar assisted heat pump system is presented in Ref. [7].

Recently, there are many reports concerning building-up, development and investigation of such hybrid installations with ground source heat pumps and solar collectors for space heating and cooling [8–15]. In all these works, solar collectors are used as an additional heat source to increase the coefficient of performance (COP) of the heat pump and to compensate the heat extraction. The systems can operate in different modes depending on the season for optimal space heating including direct solar heating and solar assisted heat pump (SAHP) heating [7–10,14]. In some of the mentioned cases, the heating is combined with producing of domestic hot water [8,9]. The switching between different working regimes is performed automatically [8]. Some investigations using experiments and long-term simulations over 20 years show that such hybrid systems with an additional heat source (solar collectors) are a good perspective for space heating with predominant heating needs [6,14]. Due to the relatively high cost of such installations, simulation studies, based mainly on using FEFLOW [16,17], TRNSYS and Matlab [18–25] software environment are often used at the design stage to optimize system performance and cost.

Almost all studies in the field of hybrid heat pump systems containing detailed experimental data describe relatively large installations, designed for district heating [18,19,21,26–28]. There are a few investigations of hybrid systems for heating of small houses

* Corresponding author.
E-mail addresses: AGeorgiev@gmx.de, agg.agg@abv.bg (A. Georgiev).

https://doi.org/10.1016/j.renene.2018.12.087
0960-1481/© 2018 Elsevier Ltd. All rights reserved.

or cottages [12] and for greenhouse heating [13]. Most of these plants are operated in Germany and Canada under climatic conditions and thermal properties of soil quite different from those in Bulgaria. There is no published detailed data on the performance of such systems in their different modes of operation in the region of Plovdiv and even all over Bulgaria. No sufficient detailed experimental data of the hybrid systems are available. This especially applies to regimes of thermal accumulation in water tanks and under the ground, as well as the relaxation after that. Detailed calculations of the energy flows between the system's components in different operation modes are also absent. Such in situ data are indispensable for the development and validation of simulation models that accurately reflect the operation of hybrid heat pump systems and provide highly effective means of designing and deploying their work under specific site conditions.

A universal hybrid thermal system with solar collectors, heat pump, water tanks and borehole heat exchangers has been constructed at the Technical University - Sofia, Plovdiv Branch [29]. It can operate in different modes of thermal energy storage and space heating. The aim of this work is to investigate experimentally five different operation regimes - two charging and three heating modes. Detailed energy analysis and comparison of the obtained data is presented as well. The collected experimental data will be used in the future to develop and validate TRNSYS simulation models of the hybrid GSHP system designed at specific for the region climate and soil conditions.

2. Design and construction of a GSHP system with solar collectors

The hybrid installation (Fig. 1) consists of the following main parts - borehole heat exchangers, a heat pump, solar collectors, water tanks and a fan coil [29]. Flat plate solar collectors are mounted on the roof just above the laboratory. They are orientated to the South and tilted at an angle of 42°. The solar part of the installation is also equipped with a 200 dm^3 hot water tank. An additional electric resistive heater of 3 kW power is mounted therein as well.

Two borehole heat exchangers (BHEs) were situated on the ground level in the area of campus 2 of TU Sofia in Plovdiv [29]. The distance between the drilled holes is 13 m, the holes' depth is 50 m and the diameter is 165 mm. During the drilling some soil samples were obtained to investigate the profile. The thermal characteristics of the soil layers near the BHE are presented in Table 1 [30].

From a geological point of view, the Plovdiv region falls into the Upper Thracian depression - a complex tectonic structure between the Rhodope massif and the Sredna Gora Mountains, where two major hydrogeological units can be separated [31]. The upper one is related to the quaternary river and proluvial deposits, where cold unconfined waters, that are connected with the rivers, are formed. The depth of the perched water is from 3 to 60 m, its direction of movement is towards the draining rivers, mainly the Maritsa River. The hydraulic conductivity is from 30 to 400 m/day and the temperature regime of the water depends on the weather conditions (normally between 12 and 14 °C). The second hydrogeological unit is the Pliocene groundwater complex located just below the quaternary aquifer. It is separated by a clay layer of variable thickness, including connections with the aquifer. The thickness of Pliocene deposits is different (10–15 to 240–360 m), reaching up to 500 m. The underground waters formed in them are pressurized. The direction of movement of the groundwater is also to the Maritsa River. The hydraulic conductivity is from 0.8 to 80 m/day. The temperature has been measured in some points at a depth of 200 m, of the order of 20 °C. Two small ground water perched layers were detected during the BHE drilling by our laboratory at depths from 10 to 15 m and 38–42 m.

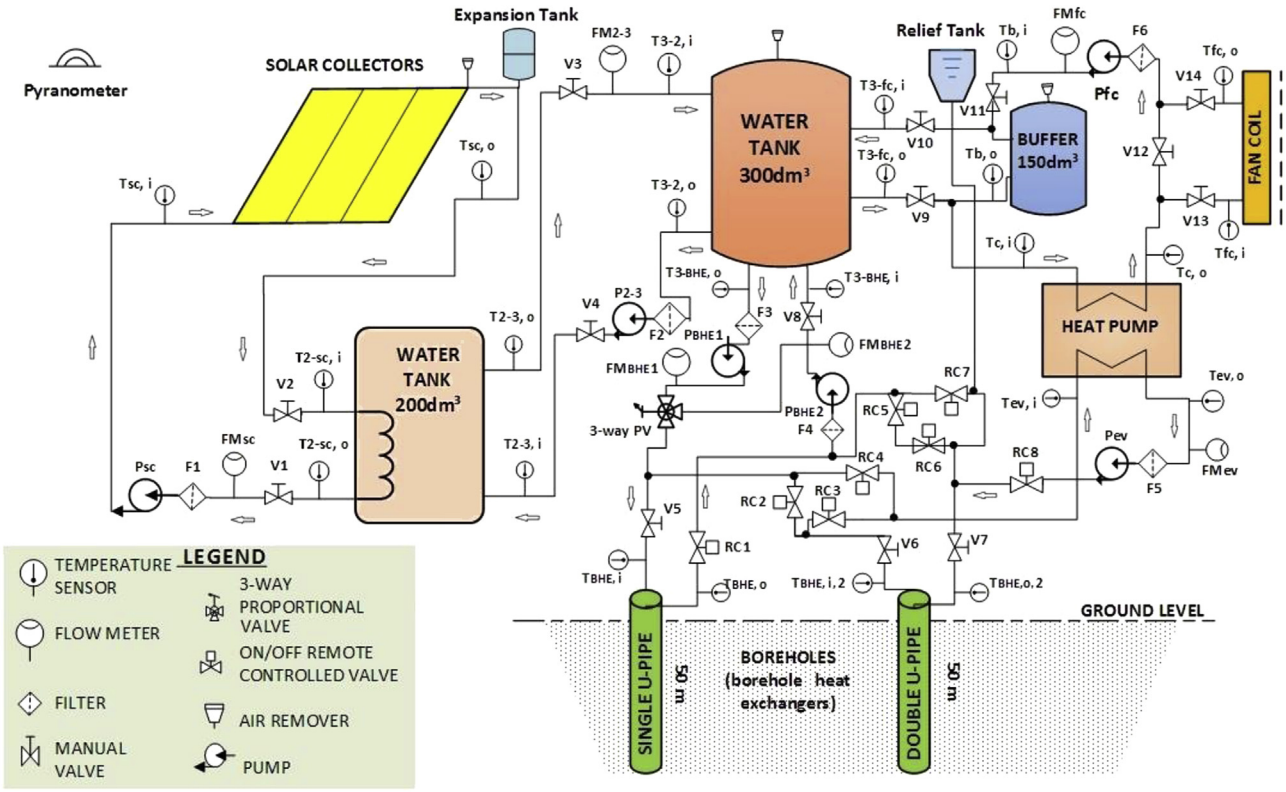

Fig. 1. Schematic diagram of the hybrid installation.

Table 1
Characteristics of the underground materials [30].

Material	Thermal conductivity	Volumetric heat capacity	Density	Depth
	W/mK	MJ/m^3	kg/m^3	m
Sandy soil	0.3	800	1600	0–0.4
Technical ground	0.83	1970	800	0.4–2.0
Clay	1.58	2000	1550	2.0–9.4
Saturated sand	2.2	2000	1480	9.4–50.0

Prior to experiments thermal response tests (TRTs) were performed to evaluate the ground thermal conductivity λ and the borehole thermal resistance R_b of the boreholes [32]. A mobile installation, earlier developed at the TU-Sofia, Plovdiv Branch, was used during the tests [33]. Tests with 7 day duration were run to evaluate thermal resistivity and conductivity of the soil and the data were calculated using a line source model (LSM). The experiments were carried out in August 2012 (with a single loop) with the following results: thermal conductivity λ = 1.65 W/mK and borehole thermal resistance R_b = 0.179 mK/W respectively.

A "Water-water" heat pump "Maxa" model HWW-A/WP 15 is situated in the laboratory. It has a nominal heating capacity of 5.9 kW, nominal cooling capacity of 4.6 kW and maximum electricity consumption of 1.2 kW [29]. Another main part of the hybrid system is the fan coil Sabiana Carisma CRC (Fig. 1). It is of air-water type and is used for space heating. There are three more water tanks in the system - a 300 dm^3 water tank, a buffer vessel with a volume of 150 dm^3 and a relief plastic tank with a volume of 20 dm^3. There are also several circulation pumps.

The measuring system contains two main parts - measuring sensors and data loggers [29]. The sensors used to measure the temperatures are of the type 3-wire RTD Pt100, class A. Six flow meters BEL90 FM1-FM6 are mounted on every circulating circuit to measure the volumetric flow rate.

A pyranometer of the type Kipp & Zonen CMP 6 is mounted in the plane of the solar collectors with the aim to measure the global solar radiation [34]. The measured values of the intensity of the solar radiation on the solar collectors often overrun at about 25% the normal values for Plovdiv (lat. long.: 42.139423, 24.772844) during the summer period (usually up to 850 ÷ 900 W/m^2). This is explained by the presence of relatively large roof panels (approximately 4 m high), where the solar collectors are located. So they act as a weak concentrator that increases the radiation on the solar collectors (respectively on the pyranometer).

A wattmeter EL-EPM02FHQ is used to measure the electricity consumption and the power of the heat pump and the water pumps with an accuracy of 0.5 W and with a range of 3.6 kW [35]. Two measuring devices are used for measurement and logging of the obtained data of the temperatures and the flow rates. The programmable Indicator TC800 performs measuring and logging of temperature by means of Pt100 with digital compensation for RTD sensor line resistance and an accuracy of 0.4% from span. The programmable Counter CT34 makes possible the measurement of the water volumetric flow rate in different circuits and the data logging on a PC. All the measuring devices are checked and calibrated immediately before the measurements to ensure the most reliable results.

3. Investigation methods of a hybrid ground source heat pump system with solar collectors

3.1. Theory

The aim of the methods is to determine the thermal characteristics of the system at different operation modes depending on the season and the heating loads. The following parameters are defined:

3.1.1. Thermal energies

The thermal energy stored in the water tanks at the end of the operation mode can be calculated as follows:

$$Q_{st} = m_{st}.c_{st}.(t_{st,end} - t_{st,in}),\ J \tag{1}$$

The injected thermal energy in the BHE during the operation mode for the time of the experiment τ_{end} can be calculated as follows:

$$Q_{inj} = \int_0^{\tau_{end}} \dot{m}_{BHE} c_{BHE}.(t_{BHE,o} - t_{BHE,i}) d\tau,\ J \tag{2}$$

The heat supplied from the fan coil to the room during the operation mode for the time of the experiment τ_{end} can be calculated as follows:

$$Q_{fc} = \int_0^{\tau_{end}} \dot{m}_{fc} c_{fc}.\left(t_{fc,i} - t_{fc,o}\right) d\tau, \tag{3}$$

The average supplied thermal energy to the evaporator during the operation mode for the time of the experiment τ_{end} can be calculated as follows:

$$Q_{ev} = \int_0^{\tau_{end}} \dot{m}_{ev} c_{ev}.(t_{ev,i} - t_{ev,o}) d\tau,\ J \tag{4}$$

The average derived thermal energy from the condenser during the operation mode for the time of the experiment τ_{end} can be calculated as follows:

$$Q_c = \int_0^{\tau_{end}} \dot{m}_c c_c.(t_{c,o} - t_{c,i}) d\tau,\ J \tag{5}$$

3.1.2. Solar collector efficiency

The efficiency of the solar collector is to be determined as a ratio of the heat flow rate extracted by the solar collector $\dot{Q}_{sc}, W$ and the solar collector area A_{ab} multiplied by the global solar insolation in the plane of the solar collectors I_{sc} [29,36]:

$$\eta_{sc} = \frac{\dot{Q}_{sc}}{A_{ab} \cdot I_{sc}}. \tag{6}$$

The heat flow rate $\dot{Q}_{sc}, W$ is defined as follows:

$$\dot{Q}_{sc} = \dot{m}_{sc} \cdot c_{sc} \cdot (t_{sc,o} - t_{sc,i}). \quad (7)$$

3.1.3. Efficiency of the borehole heat exchanger (BHE)

The efficiency of the BHE is to be determined as a ratio of thermal energy extracted from the BHE to thermal energy injected in the BHE for a period of time (annual or seasonal) [29,37]:

$$\eta_{BHE} = \frac{Q_{ext}}{Q_{inj}}, \quad (8)$$

where Q_{ext} is thermal energy extracted from the BHE, J;

Q_{inj} - thermal energy injected in the BHE, J.

Let us assume that the BHE temperature returns to the same value after a period of time (for example one year). So the BHE efficiency can be determined as follows:

$$\eta_{BHE} = \frac{Q_{ext}}{Q_{ext} + Q_{loss}} = 1 - \frac{Q_{loss}}{Q_{inj}}, \quad (9)$$

where Q_{loss} are BHE heat losses for a period of time, J,

$Q_{inj} = Q_{ext} + Q_{loss}$.

3.1.4. Efficiencies of the hybrid system at different operational modes

3.1.4.1. Charging mode of the water storages with thermal energy from the solar collectors. The system efficiency is to be determined in this mode as a ratio of stored thermal energy in the water accumulators to global solar insolation in the plane of the solar collectors plus electrical power of the circulation pumps during the test period:

$$\eta_{s,1} = \frac{m_{st} . c_{st} . (t_{st,end} - t_{st,in})}{\sum_{i=1}^{n} \int_0^{\tau_i} (I_{sc} . A_{ab} + N_{sc}) d\tau + \int_0^{\tau_{end}} N_{2-3} . d\tau}. \quad (10)$$

3.1.4.2. Charging mode of borehole heat exchanger (BHE) with thermal energy from the solar collectors. The system efficiency is to be determined in this mode as a ratio of thermal energy injected to the BHE to global solar insolation in the plane of the solar collectors plus electrical powers of the circulation pumps during the test period:

$$\eta_{s,2} = \frac{\int_0^{\tau_{end}} \dot{m}_{BHE} . c_{BHE} . (t_{BHE,i} - t_{BHE,o}) d\tau}{\sum_{i=1}^{n} \int_0^{\tau_i} (I_{sc} . A_{ab} + N_{sc}) d\tau + \int_0^{\tau_{end}} N_{2-3} d\tau + \int_0^{\tau_{end}} N_{BHE} d\tau} \quad (11)$$

3.1.4.3. Direct solar heating mode. The system efficiency is to be determined in this mode as a ratio of thermal energy supplied to the air convector to global solar insolation in the plane of the solar collectors plus electrical powers of the circulation pumps during the test period:

$$\eta_{s,3} = \frac{\int_0^{\tau_{end}} \dot{m}_{fc} . c_{fc} . \left(t_{fc,i} - t_{fc,o}\right) d\tau}{\sum_{i=1}^{n} \int_0^{\tau_i} (I_{sc} . A_{ab} + N_{sc}) d\tau + \int_0^{\tau_{end}} \left(N_{2-3} + N_{fc}\right) d\tau} \quad (12)$$

3.1.4.4. Heating mode with ground source heat pump (GSHP). The system efficiency is to be determined in this mode as a ratio of thermal energy supplied to the fan coil and thermal energy extracted from the BHE plus electrical powers of the heat pump and the circulation pumps during the test period:

$$\eta_{s,4} = \frac{\int_0^{\tau_{end}} \dot{m}_{fc} . c_{fc} . \left(t_{fc,i} - t_{fc,o}\right) d\tau}{\int_0^{\tau_{end}} N_{fc} . d\tau + \sum_{j=1}^{m} \int_0^{\tau_j} \{\dot{m}_{BHE} . c_{BHE} (t_{BHE,o} - t_{BHE,i}) + N_{BHE}\} d\tau + \sum_{k=1}^{m} \int_o^{\tau_k} N_{hp} . d\tau} \quad (13)$$

3.1.4.5. Heating mode with solar assisted heat pump (SAHP). The system efficiency is to be determined in this mode as a ratio of thermal energy supplied to the fan coil to global solar insolation in the plane of the solar collectors plus electrical powers of the heat pump and the circulation pumps during the test period:

$$\eta_{s,5} = \frac{\int_0^{\tau_{end}} \dot{m}_{fc} . c_{fc} . \left(t_{fc,i} - t_{fc,o}\right) d\tau}{\sum_{i=1}^{n} \int_0^{\tau_i} (I_{sc} . A_{ab} + N_{sc}) d\tau + \sum_{l=0}^{p} \int_0^{\tau_l} N_{AES} d\tau + \int_0^{\tau_{end}} \left(N_{2-3} + N_{fc} + N_{ev}\right) d\tau + \sum_{f=0}^{q} \int_0^{\tau_f} N_{hp} d\tau}, \quad (14)$$

where: m_{st} is the water mass in the storages, kg;

$\dot{m}_{BHE}$, $\dot{m}_{fc}$, $\dot{m}_{ev}$, $\dot{m}_c$, $\dot{m}_{sc}$ - average fluid mass flow rate through BHE, fan coil, evaporator, condenser and solar collectors, kg/s;
c - average fluid mass specific heat capacity, J/kgK;
$t_{st,end}$, $t_{st,in}$ - end and initial water temperatures in the storage, °C;
$t_{BHE,i}$, $t_{BHE,o}$ - inlet and outlet fluid BHE temperatures, °C;
$t_{fc,i}$, $t_{fc,o}$ - inlet and outlet fluid fan coil temperature, °C;
$t_{ev,i}$, $t_{ev,o}$ - inlet and outlet fluid evaporator temperatures, °C;
$t_{c,i}$, $t_{c,o}$ - inlet and outlet fluid condenser temperatures, °C;
A_{ab} - solar collector absorber area, m^2;
I_{sc} - intensity of the global solar radiation in plane of the solar collectors, W/m^2;
N_{sc}, N_{2-3} - momentary power of the solar circuit pump and the power of the pump between the 200 dm^3 and 300 dm^3 tanks, W;
N_{BHE} - momentary power of the BHE circuit pump, W;
N_{fc} - momentary power of the fan coil water circuit pump, W;
N_{hp} - momentary electrical power of the heat pump during its operation period, W;
N_{ev} — momentary electrical power of the evaporator circuit pump, W;
N_{AES} - momentary electrical power of the AES (electrical heater), W;
n - activity period number of the solar circuit pump,-;
τ_i - i—th time period of the solar circuit pump operation, s;
τ — time (it is 0 at the experiment start), s;
$\Delta\tau$ - time step between two consecutive measurements, s;
τ_{end} - time at the experiment's end, s;
m — activity period number of the heat pump and the BHE circuit pump in GSHP operation mode,-;
τ_j - j—th time period of the BHE circuit pump operation, s;
τ_k - k—th time period of the heat pump operation in GSHP operation mode, s;
τ_l - l—th time period of the AES operation (electrical heater), s;
p - activity period number of the AES,-;
q - activity period (cycles) number of the heat pump operation in SAHP mode,-;
τ_f - f—th time period of the heat pump operation in SAHP mode, s.

3.2. Investigation procedure

The measurements are made under quasi-stationary conditions:

- all parameters are measured simultaneously every minute during the measuring period;
- the tested solar collectors are oriented towards the sun and tilted to the horizon at an angle $(\varphi - \delta)$.

3.3. Accuracy of the measured parameters

The acceptable deviations of the directly measured parameters are as follows:

- intensity of the global solar insolation - ± 2%;
- temperatures - ± 2%;
- volume flow rates - ± 2%;
- electrical powers - ± 5%.

The acceptable deviations of the indirectly measured parameters are as follows:

- solar collector heat flow rate - ± 6%;
- solar collector efficiency - ± 6%;
- system efficiency by different operation modes - ± 6%.

4. Experimental results and discussion

4.1. Operation modes

The hybrid installation (Fig. 1) can operate in 5 different modes depending on the seasonal conditions and the needed load as follows [29]:

1. Charging of water tanks with thermal energy from solar collectors (CWT mode): solar collectors charge a water storage with thermal energy.
2. Charging of borehole thermal energy storage (BTES) with thermal energy from solar collectors (CBTES mode): solar collectors charge the boreholes with thermal energy.
3. Direct solar heating (DSH mode): a thermal energy from water tank is delivered directly to the consumer.
4. GSHP heating (GSHPH mode): heat is delivered to the heat pump evaporator from the boreholes.
5. Heating with SAHP (SAHPH mode): heat is delivered to the heat pump evaporator from the solar collectors.

4.2. Charging of water tanks with thermal energy from solar collectors (CWT mode)

4.2.1. Test conditions

The simplified working scheme of the mode is presented in Fig. 2. The test conditions of the CWT mode are presented in Table 2.

4.2.2. Operation results and energy diagram of CWT mode

An experiment was performed on the installation in CWT mode (Fig. 2). It was carried out under the test conditions presented in Table 2. The energy flows between the system components in this mode are shown in Fig. 3. All the presented values are calculated on the basis of data obtained during the experiment.

The heat flow rate extracted by the solar collector $\dot{Q}_{sc}$, is calculated by using Eq. (7) from the Investigation methods (chapter 3.1). The fluid mass flow rate through the solar collector $\dot{m}_{sc}$ is determined taking into account the activity of the pump in the solar circuit. The inlet and outlet fluid solar collector temperatures $t_{sc,i}$ and $t_{sc,o}$ are measured in every step $\Delta\tau = 1$ min. The sum of the heat calculated for every step is the total heat gained from the solar collectors $Q_{SC} = 59\ 150$ kJ (Fig. 3).

The global solar insolation intensity in the plane of the solar collectors I_{sc} is measured every minute, too. The final value of the thermal energy from the sun is 105 193 kJ (Fig. 3). The integral electrical consumption of the solar circuit pump Q_{PSC} is measured during the test and has the value of 1 270 kJ (Fig. 3). The value of 47 313 kJ is the heat loss due to reflection and the proper absorption of SCs (Fig. 3).

The measured temperatures between both water tanks have very similar values. That is why the 200 dm^3 and the 300 dm^3 tanks can be considered a common water storage with a volume of 500 dm^3. Thus the two tanks will be considered in the next modes as 500 dm^3 integral tank.

The thermal energy stored in the water tanks at the end of the CWT mode can be calculated by means of Eq. (1) and its value is 37 999 kJ. The integral electrical consumption of the pump between the 200 dm^3 and 300 dm^3 tanks $Q_{P2\text{-}3}$ is measured during the test

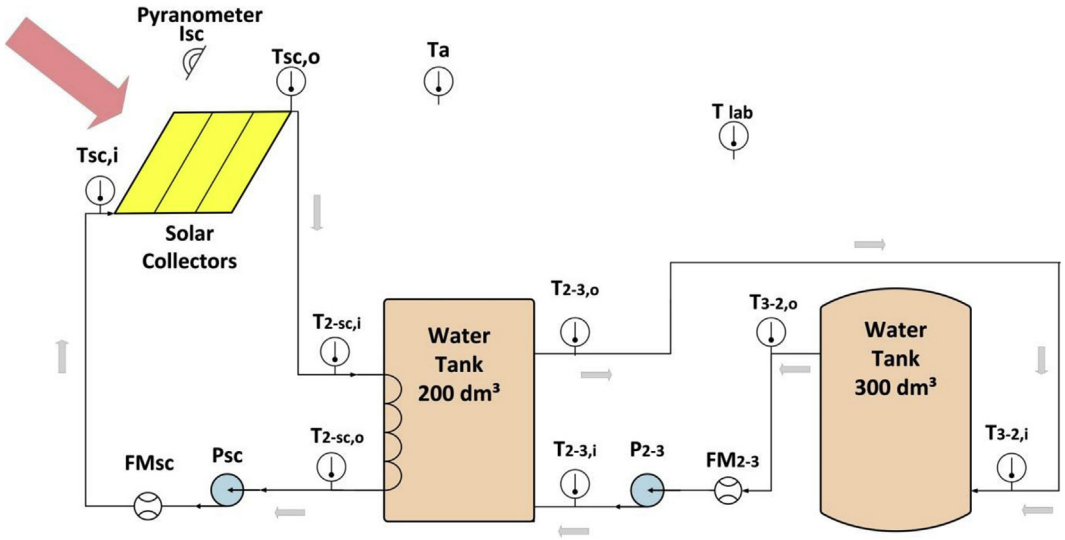

Fig. 2. Working scheme of the hybrid installation in CWT mode.

Table 2
Test conditions of CWT mode.

Experiment time period	02.09÷05.09.2014
Experiment duration	4349min (about 3 days)
Working fluid in the solar circuit	water
Initial water tanks temperature	25.75 °C (measured with sensor $T_{3-2,o}$)
Total water amount in the tanks	500 dm^3
Slope angle of the solar collectors	42° ± 2°
Total area of the solar collectors	6.45m^2
Pyranometer position	in the plane of the solar collectors
Time interval of the logging measuring data	1min

and has the value of 10 310 kJ (Fig. 3). Finally the value of 31 461 kJ is equal to the heat losses from the water tanks (Fig. 3). The system efficiency at CWT mode is determined by means of Eq. (10) from the Investigation methods (chapter 3.1) and has the value $\eta_{s,1} = 32.56\%$.

4.3. Charging of borehole thermal energy storage (BTES) with thermal energy from solar collectors (CBTES mode)

4.3.1. Test conditions

The simplified working scheme in this mode is presented in Fig. 4. The test conditions of the CBTES mode are presented in Table 3.

4.3.2. Operation results and energy diagram of CBTES mode

An experiment was conducted on the installation in CBTES mode (Fig. 4). It was carried out under the test conditions presented

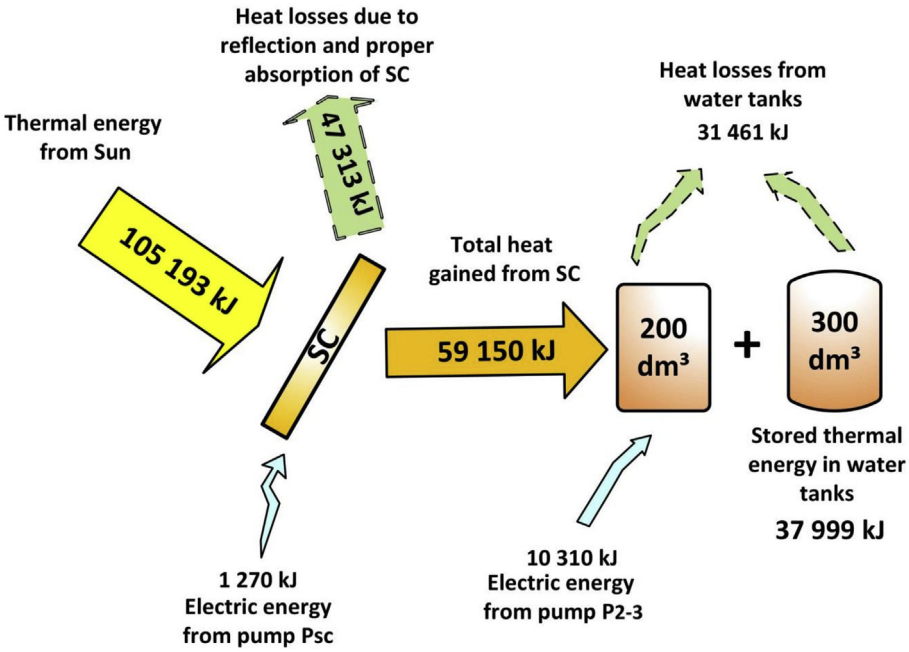

Fig. 3. Energy diagram of CWT mode.

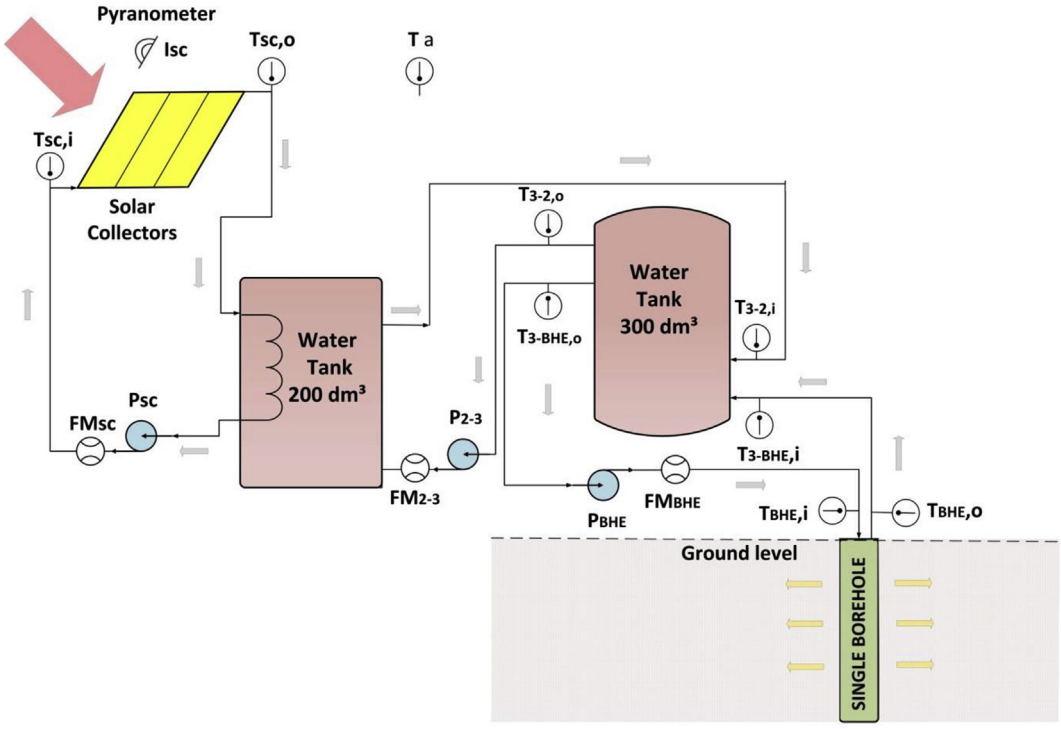

Fig. 4. Working scheme of the hybrid installation in CBTES mode.

Table 3
Test conditions of CBTES mode.

Experiment time period	23.09. ÷ 23.10.2014
Experiment duration	42845min (about 1 month)
Working fluid in the solar circuit	water
Working fluid in the BHE circuit	water
Tested borehole	single BHE
Initial water tanks temperature	25.75 °C (measured with sensor $T_{3\text{-}2,o}$)
Initial water temperature in 300 dm³ tank	39.9 °C (measured with sensor $T_{3\text{-}BHE,o}$)
Total water amount in the tanks	500 dm³
Slope angle of the solar collectors	42°±2°
Total area of the solar collectors	6.45m²
Pyranometer position	in the plane of the solar collectors
Undisturbed ground temperature	14.3 °C
Time interval of the logging measurement data	1min

in Table 3. The energy flows between the system components in this mode are shown in Fig. 5. All the presented values are calculated on the basis of data obtained during the experiment.

The determination of the total heat gained from the solar collectors is carried out using the methods presented in chapter 4.2.2, it is $Q_{sc} = 1475\ 359$ kJ (Fig. 5). Following similar methods as that in chapter 4.2.2, the final value of the thermal energy from the sun is calculated equal to 2581 965 kJ (Fig. 5). The integral electrical consumption of the solar circuit pump Q_{Psc} is measured during the test and has the value of 21 582 kJ (Fig. 5). The final value of 1128 188 kJ is equal to the heat losses due to the reflection and proper absorption of SCs (Fig. 5).

The integral electrical consumption of the pump between the tanks of 200 dm³ and 300 dm³ $Q_{P2\text{-}3}$ is measured during the test and has the value of 97 685 kJ (Fig. 5). The integral electrical consumption of the BHE circuit pump $Q_{P,BHE}$ is measured, as well. Its value during the CBTES mode is 113 111 kJ (Fig. 5).

The injected thermal energy in the BHE during the CBTES mode for the time of the experiment τ_{end} can be calculated by means of Eq. (2) and its value is 1463 526 kJ (Fig. 5). Thus the injected thermal energy in the BHE during the CBTES mode per meter is 29 270.5 kJ/m (the depth of the BHE is 50 m). The final value of 1350 415 kJ is the thermal energy stored in the water tanks during the CBTES mode (Fig. 5). The value of 222 629 kJ is equal to the heat losses from the water tanks (Fig. 5). The system efficiency at CBTES mode is determined by means of Eq. (11) from the Investigation methods (chapter 3.1) and has the following value $\eta_{s,2} = 52.0\%$.

Fig. 6 shows the temperature difference between the outlet $t_{BHE,o}$ and the inlet $t_{BHE,i}$ fluid BHE temperatures as a function of time (min). The variation of the temperature difference during the different time periods is visualized.

The injected heat flow rate to the BHE as a function of time (min) is presented in Fig. 7. The variations of the injected energy for the different time periods are well pronounced.

The BHE temperatures at a depth of 1, 10, 20, 30, 40 and 50 m are measured, too. Fig. 8 shows the BHE temperature at a depth of 50 m. The trend of the temperature rise with time is presented (it is obviously that the ground temperature increases with 1–2 °C during the charging mode).

After charging of the BHE during the CBTES mode for about a month, the thermal relaxation of the ground near the BHE was studied (the temperatures in depth of the BHE were measured for 4 days). The results are presented in Fig. 9 (ambient temperature is presented, too).

4.4. Direct solar space heating (DSH mode)

4.4.1. Test conditions

The simplified working scheme of the mode is presented in Fig. 10. The test conditions of the DSH mode are presented in Table 4.

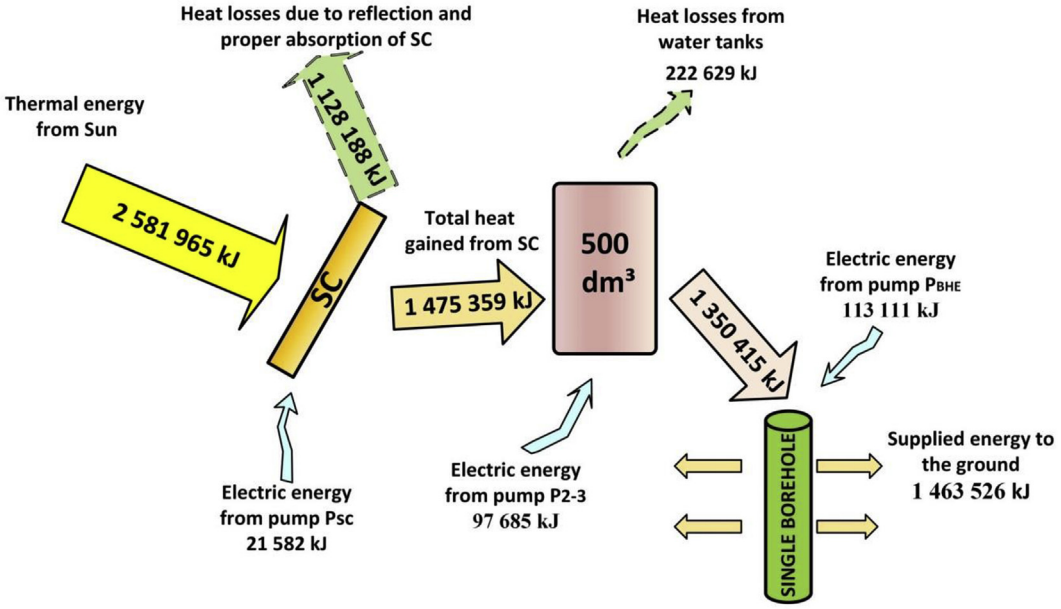

Fig. 5. Energy diagram of CBTES mode.

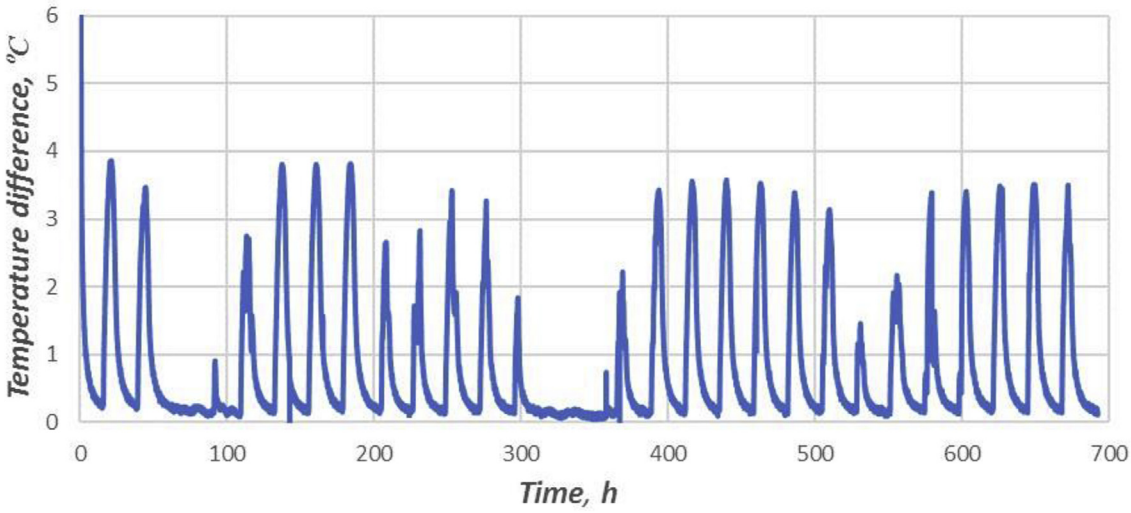

Fig. 6. Temperature difference between the outlet $t_{BHE,o}$ and the inlet $t_{BHE,i}$ fluid BHE temperatures.

4.4.2. Operation results and energy diagram of the DSH mode

An experiment was performed on the installation in DSH mode (Fig. 10). It was made under the test conditions presented in Table 4. The energy flows between the system components in this mode are shown in Fig. 11. All the presented values are calculated on the basis of data obtained during the experiment.

The fluid mass flow rate through the solar collector $\dot{m}_{sc}$ is determined taking into account the activity of the pump in the solar circuit. The inlet and outlet fluid solar collector temperatures $t_{sc,i}$ and $t_{sc,o}$ are measured for every step $\Delta\tau = 1$min. The sum of the heat calculated for every step is the total heat gained from the solar collectors $Q_{SC} = 156\,905$ kJ (Fig. 11). The global solar insolation intensity in the plane of the solar collectors I_{sc} is measured every minute, too. The final value of the thermal energy from the sun is 311 424 kJ (Fig. 11). The integral electrical consumption of the solar circuit pump $Q_{P,SC}$ is measured during the test and has the value of 2 701 kJ (Fig. 11). The final value of 157 220 kJ is equal to the heat losses due to the reflection and proper absorption of SCs (Fig. 11).

The integral electrical consumption of the pump between the tanks of 200 dm^3 and 300 dm^3 $Q_{P,2\text{-}3}$ is measured during the test and has the value of 12 660 kJ (Fig. 11). The integral electrical consumption of the fan coil water circuit pump - $Q_{P,fc}$ was measured, too. Its value during the DSH mode is 1 999 kJ (Fig. 11). The fluid mass flow rate through the consumer $\dot{m}_{fc}$ is determined, too. The heat supplied from the fan coil to the room during the DSH mode for the time of the experiment τ_{end} can be calculated by means of Eq. (3) and its value is 159 776 kJ (Fig. 11). The final value of 157 777 kJ is the thermal energy stored in the water tanks during the DSH mode (Fig. 11). The value of 11 788 kJ is equal to the heat losses from the water tanks (Fig. 11). The system efficiency at DSH mode is determined by means of Eq. (12) from the Investigation methods (chapter 3.1) and has the following value $\eta_{s,3} = 48.59\%$. Fig. 12 shows the inlet $t_{fc,i}$, and outlet $t_{fc,o}$ fluid fan coil temperatures as a function of time (min).

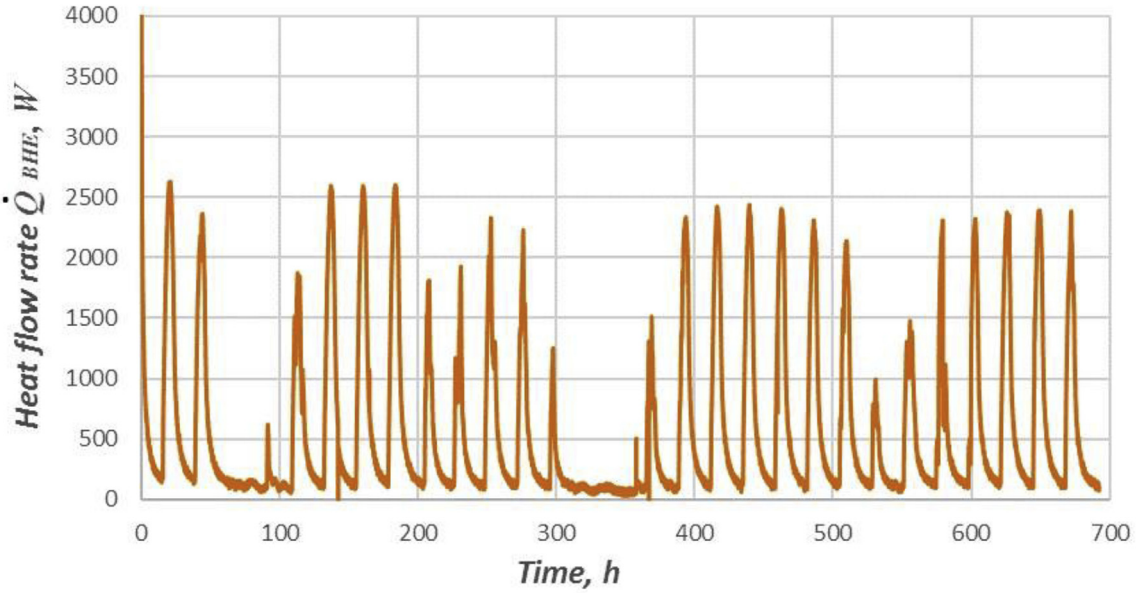

Fig. 7. Injected heat flow rate to the borehole heat exchanger.

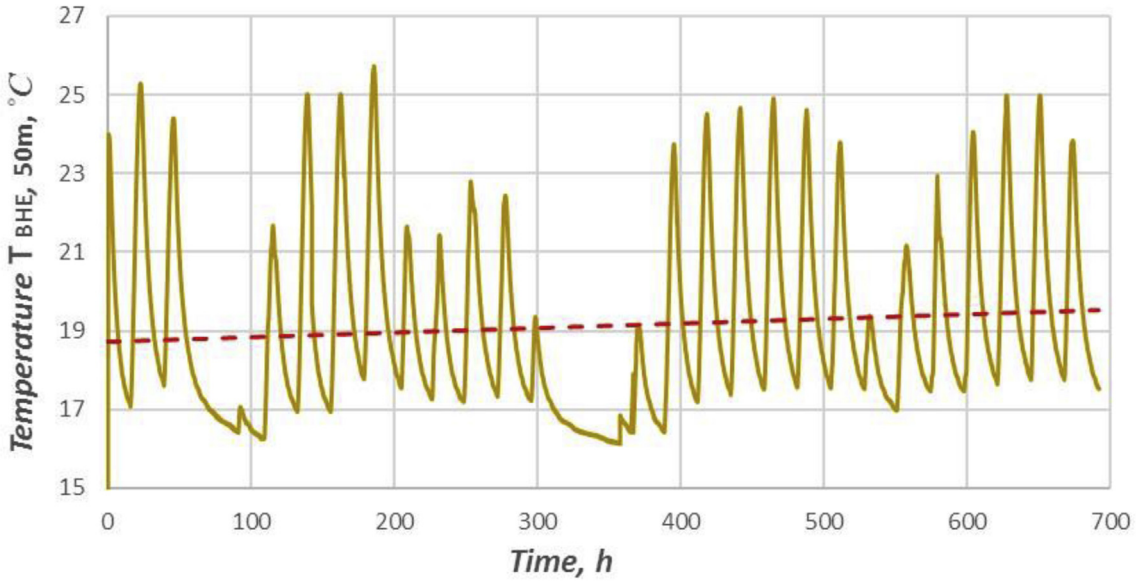

Fig. 8. Borehole heat exchanger temperature at a depth of 50 m with trend of the temperature growth.

4.5. Ground source heat pump space heating (GSHPH mode)

4.5.1. Test conditions

The simplified working scheme of the mode is presented in Fig. 13. The test conditions of the GSHPH mode are presented in Table 5.

4.5.2. Operation results and energy diagram of the GSHPH mode

An experiment was performed on the installation in GSHPH mode (Fig. 13). It was made under the test conditions presented in Table 5. The energy flows between the system components in this mode are shown in Fig. 14. All the presented values are calculated on the basis of data obtained during experiment.

The fluid mass flow rate through the evaporator $\dot{m}_{ev}$ is determined taking into account the activity of the pump in the evaporator circuit. The average supplied thermal energy to the evaporator during the GSHPH mode for the time of the experiment τ_{end} can be calculated by means of Eq. (4) and its value is 2 324 058 kJ (Fig. 14).

The fluid mass flow rate through the HP condenser $\dot{m}_c$ is determined taking into account the activity of the pump in the condenser circuit. The average derived thermal energy from the condenser during the GSHPH mode for the time of the experiment τ_{end} can be calculated by means of Eq. (5) and its value is 3978 698 kJ (Fig. 14).

The integral electrical consumption of the evaporator circuit pump $Q_{P,ev}$ is measured during the test and has the value of 264 456 kJ (Fig. 14). The integral electrical consumption of the fan coil water circuit pump $Q_{P,fc}$ was measured, too. Its value during the GSHPH mode is 137 772 kJ (Fig. 14). The integral electrical

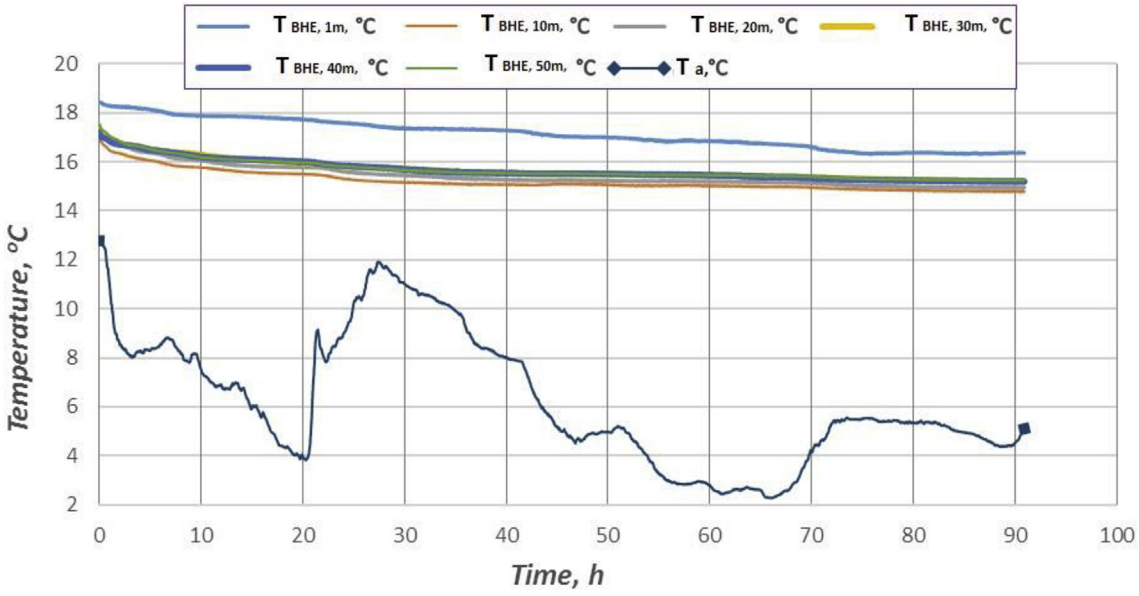

Fig. 9. Temperatures in depth of the BHE and ambient temperature.

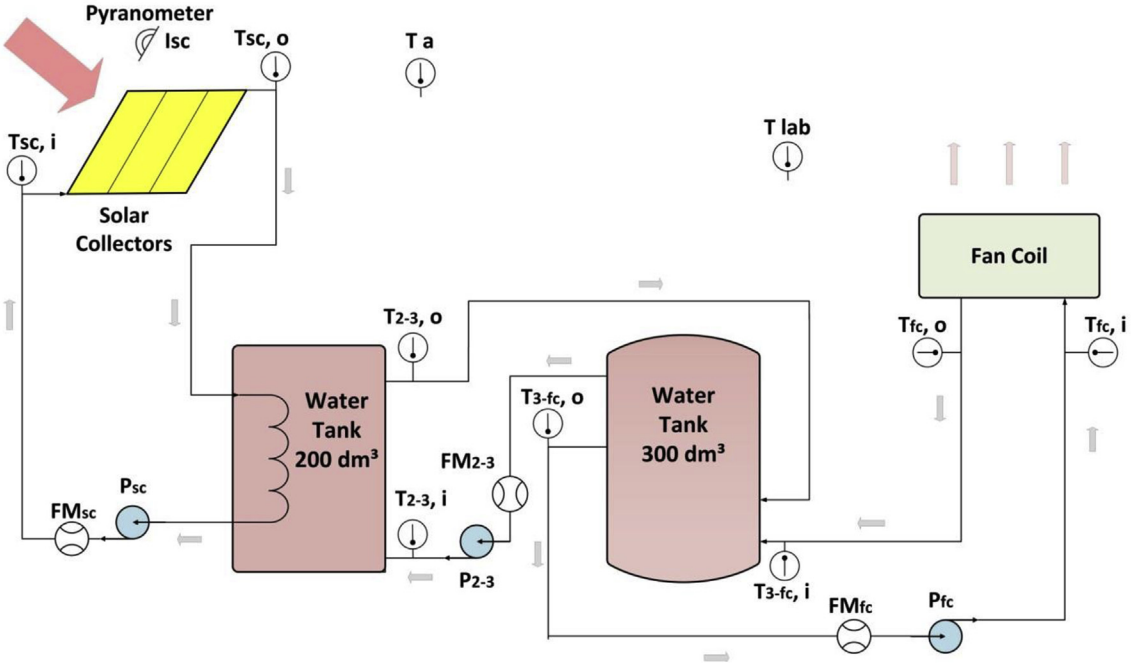

Fig. 10. Working scheme of the hybrid installation in DSH mode.

Table 4
Test conditions of DSH mode.

Experiment time period	05.09. ÷ 09.09.2014
Experiment duration	5553 min (about 5 days)
Working fluid in the solar circuit	water
Initial water tanks temperature	43.05 °C (measured with sensor $T_{3\text{-}fc,o}$)
Total water amount in the tanks	500 dm^3
Slope angle of the solar collectors	42°±2°
Total area of the solar collectors	6.45m^2
Position of the pyranometer	in the plane of the solar collectors
Time interval of the logging measurement data	1 min
Fan coil	continuous work, air flow rate of 535 m^3/h

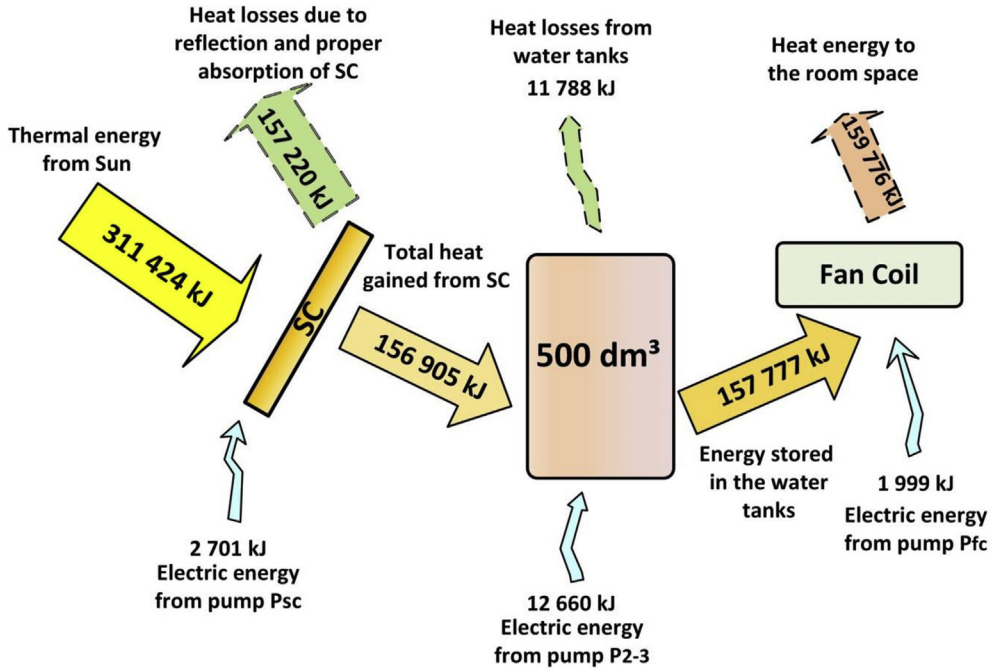

Fig. 11. Energy diagram of DSH mode.

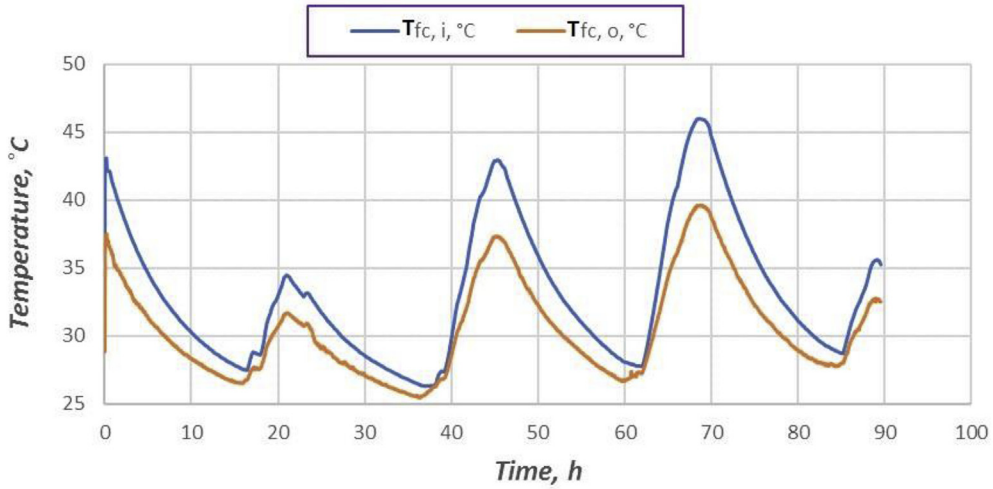

Fig. 12. Inlet $t_{fc,i}$ and outlet $t_{fc,o}$ fluid fan coil temperatures during DSH mode.

consumption of the heat pump compressor Q_{hp} was measured as 1490 184 kJ (Fig. 14). The value of 100 000 kJ is equal to the heat losses from the heat pump (Fig. 14).

The fluid mass flow rate through the fan coil $\dot{m}_{fc}$ is determined taking into account the activity of the pump in the fan coil circuit. The heat supplied from the fan coil to the room during the GSHPH mode for the time of the experiment τ_{end} can be calculated using Eq. (3). The calculated value is 4067 083 kJ (Fig. 14). The final value of 3929 311 kJ is the thermal energy stored in the buffer tank during the GSHPH mode (Fig. 14). The value of 49 387 kJ is the heat loss from the buffer tank (Fig. 14). The system efficiency at GSHPH mode is determined by means of Eq. (13) from the Investigation methods (chapter 3.1) and has the following value $\eta_{s,4} = 96.46\%$.

The BHE temperatures at a depth of 1, 10, 20, 30, 40 and 50 m are measured, too. Fig. 15 shows the BHE temperature at a depth of 50 m. The trend of the temperature rise with time is presented there (the observed gradual decrease in the mean ground temperature at the BHE during the studied period is within the range of 1.85 ÷ 1.25 °C).

Immediately after extracting heat energy by means of a heat pump during the GSHPH mode (about 1 month), the thermal relaxation of the ground near the BHE was studied (the temperatures in depth of the BHE were measured during the next 5 days, 117 h). The results are presented in Fig. 16 (the ambient temperature is shown, too).

4.6. Solar assisted heat pump heating (SAHPH mode)

4.6.1. Test conditions

The simplified working scheme of the mode is presented in

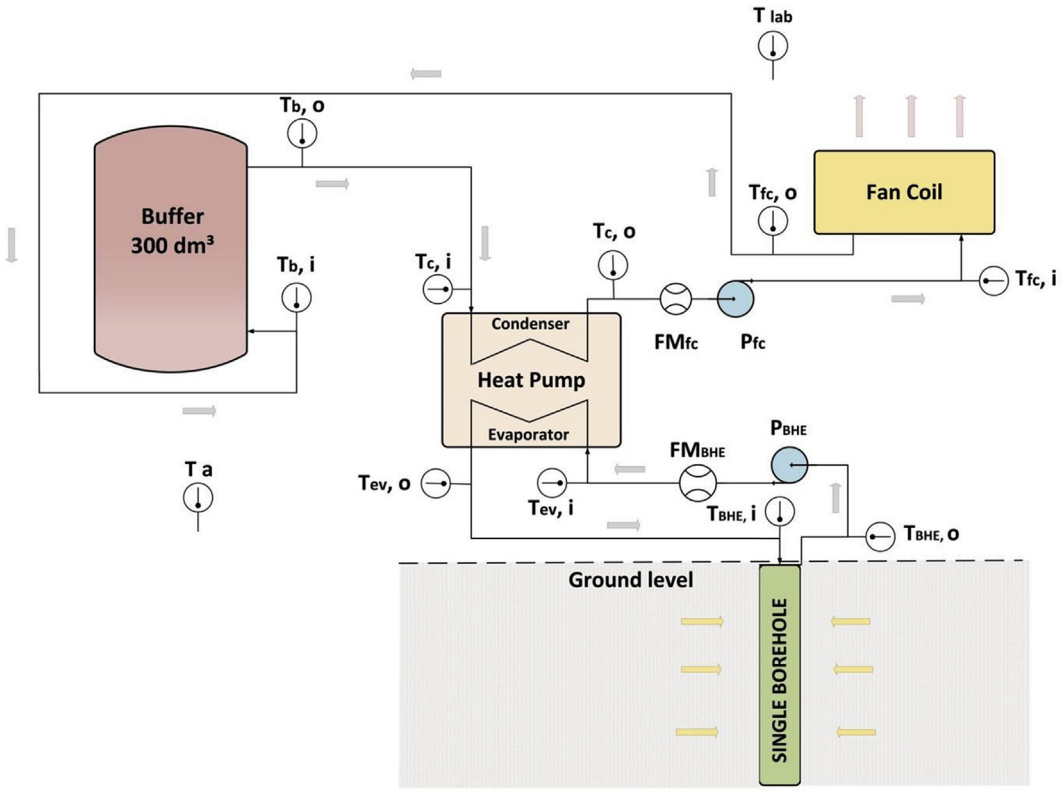

Fig. 13. Working scheme of the hybrid installation in GSHPH mode.

Table 5
Test conditions of GSHPH mode.

Experiment time period	17.11.÷15.12.2014
Experiment duration	40285 min (about 28 days)
Tested BHE	with single U-tube (single BHE)
Undisturbed ground temperature	14.01 °C
Working fluid in the BHE circuit	water
Buffer vessel	300 dm^3 water tank
Initial water temperature in the buffer	33.16 °C (measured with sensor $T_{3\text{-}fc,o}$)
Time interval of the logging measuring data	1 min
Fan coil	continuous work with air flow rate of 655 m^3/h
Minimal outlet fluid condenser temperature	35 °C
Maximal outlet fluid condenser temperature	43 °C
Minimal inlet fluid evaporator temperature	3 °C

Fig. 17. The test conditions of the SAHPH mode are presented in Table 6.

4.6.2. Operation results and energy diagram of the SAHPH mode

An experiment was performed on the installation in SAHPH mode (Fig. 17). It was made under the test conditions presented in Table 6. The energy flows between the system components in this mode are shown in Fig. 18. All the presented values are calculated on the basis of data obtained during experiment.

The determination of the total heat gained from the solar collectors is made after the methods presented in chapter 4.2.2, it is $Qsc = 21\,778$ kJ (Fig. 18). Following a similar method like in chapter 4.2.2, the final value of the thermal energy from the sun is calculated equal to 54 839 kJ (Fig. 18). The integral electrical consumption of the solar circuit pump $Q_{P,sc}$ is measured during the test and has the value of 790 kJ (Fig. 18). The value of 33 851 kJ is equal to the heat losses due to the reflection and proper absorption of SCs (Fig. 18).

The integral electrical consumption of the pump between the tanks of 200 dm^3 and 300 dm^3 $Q_{P2\text{-}3}$ is measured during the test and has the value of 9 941 kJ (Fig. 18). The integral electrical consumption of the evaporator circuit pump - $Q_{P,ev}$ is measured during the test and has the value of 7 643 kJ (Fig. 18). The integral electrical consumption of the fan coil water circuit pump - $Q_{P,fc}$ was measured, too. Its value during the SAHPH mode is 18 312 kJ (Fig. 18).

An electric resistive heater (3 kW) is used as additional energy source mounted in the 200 dm^3 tank. It is used to simulate additional solar collector area because of the insufficiency heat produced by the SCs during the day in this mode. Its integral electrical consumption Q_{AES} is 273 520 kJ (the kept water tank temperature was 23 ÷ 27 °C) (Fig. 18). The integral electrical consumption of the heat pump compressor Q_{hp} was measured as 131 908 kJ.

The determination of the average supplied thermal energy to the evaporator during the SAHPH mode for time of the experiment τ_{end} is made after the methods presented in chapter 4.5.2, it is

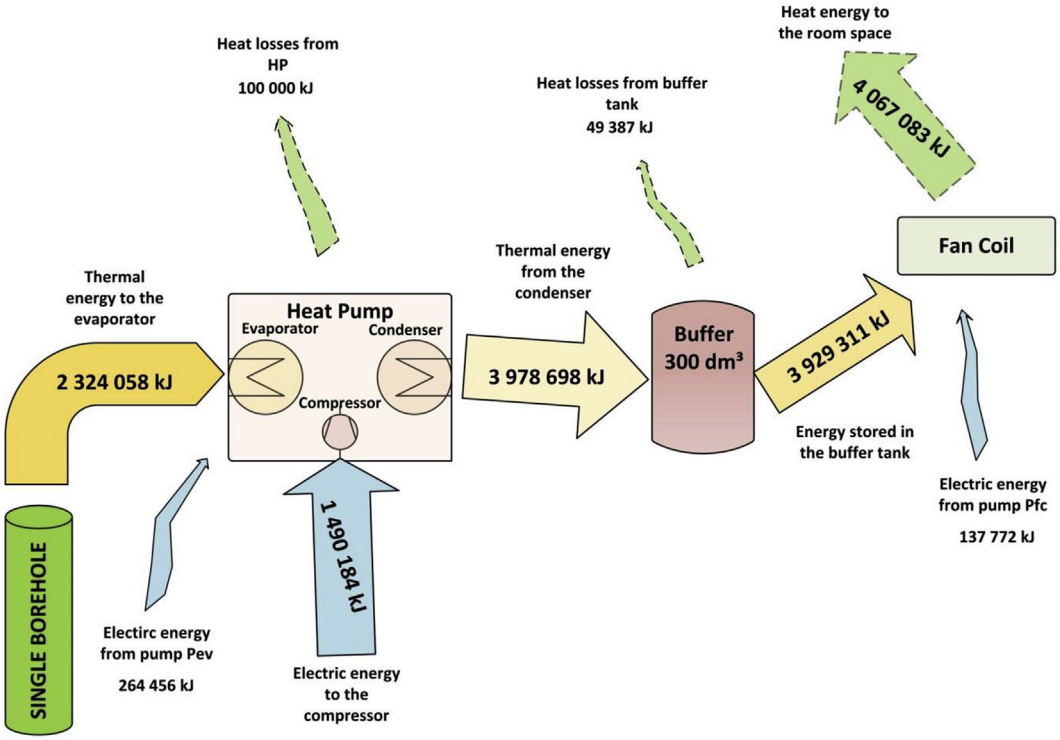

Fig. 14. Energy diagram of GSHPH mode.

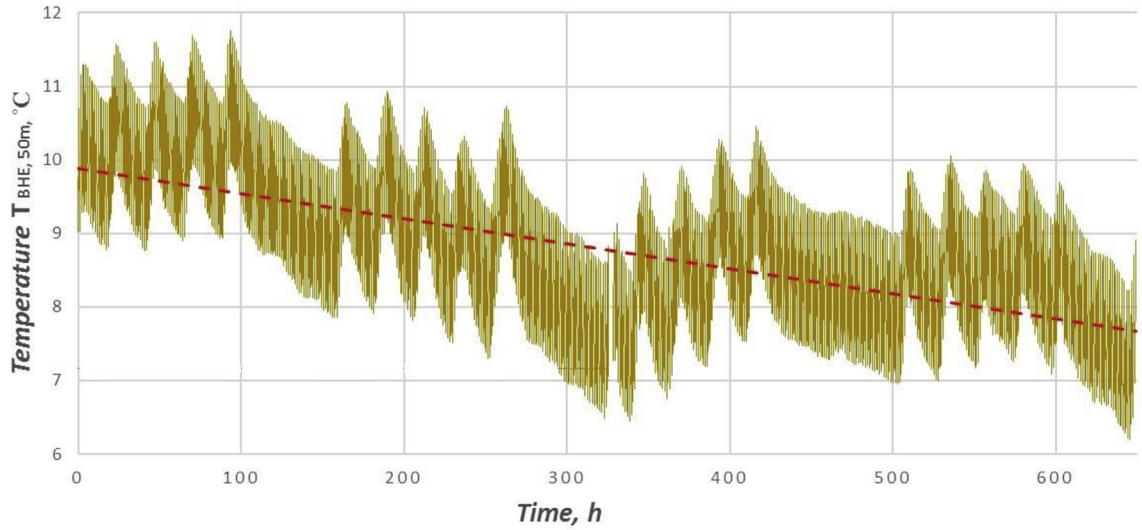

Fig. 15. Borehole heat exchanger temperature at a depth of 50 m with trend of the temperature decrease.

$Qev = 295\ 249$ kJ (Fig. 18). The value of 9 990 kJ is the heat loss from the water tanks (Fig. 18).

The determination of the average supplied thermal energy to the condenser during the SAHPH mode for the time of the experiment τ_{end} is made after the methods presented in chapter 4.5.2, it is $Qc = 430\ 665$ kJ (Fig. 18). The received value of 4 135 kJ is the heat loss from the water tanks (Fig. 18).

The fluid mass flow rate through the fan coil $\dot{m}_{fc}$ is determined taking into account the activity of the pump in the fan coil circuit. The heat supplied from the fan coil to the room during the SAHPH mode for the time at the experiment τ_{end} can be calculated using Eq. (3). The calculated value is 444 621 kJ (Fig. 18). The final value of 426 309 kJ is the thermal energy stored in the buffer tank during the SAHPH mode (Fig. 18). The value of 4 356 kJ is the heat loss from the buffer tank (Fig. 18). The system efficiency at SAHPH mode is determined by means of Eq. (14) from the Investigation methods (chapter 3) and has the following value $\eta_{s.5} = 97.95\%$.

4.7. Error analysis

There are three types of errors, which can occur during an experiment: systematic, occasional and dynamic errors. There were no systematic errors during the tests because all the measuring instruments were calibrated recently before starting the

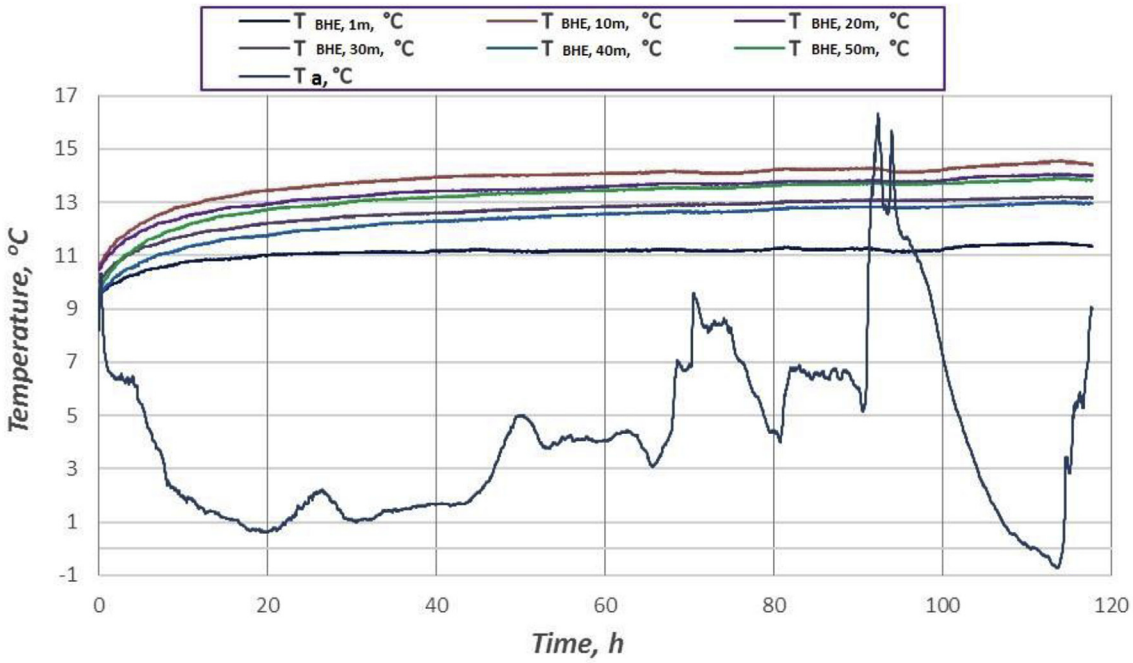

Fig. 16. Temperatures in depth of the BHE and the ambient temperature.

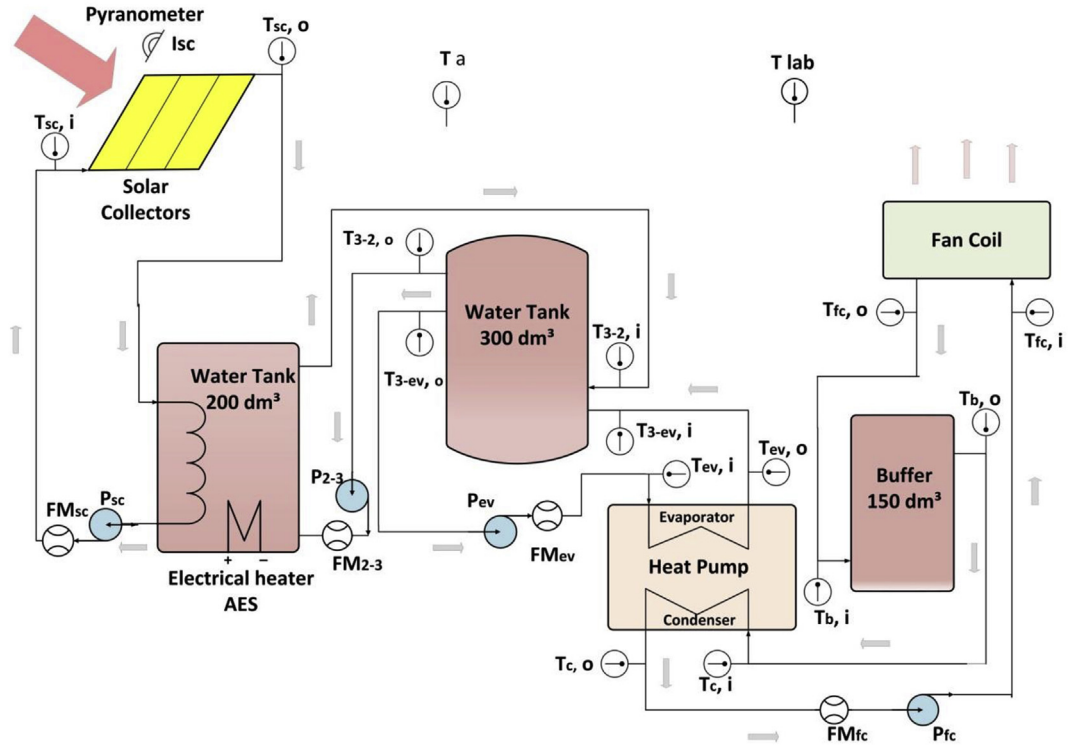

Fig. 17. Working scheme of the hybrid installation in SAHPH mode.

measurements. Dynamic errors during the experiment were not present for the following reasons:

- the measuring equipment was used in the acceptable working condition limits of the instruments;
- the installation operated for more than an hour before starting the reading.

The occasional errors were evaluated by means of regression analysis. Seven linear models were created for the solar collector efficiency η_{sc}, the coefficient of performance of the heat pump COP_{hp} and the five system efficiencies $\eta_{s,1}$, $\eta_{s,2}$, $\eta_{s,3}$, $\eta_{s,4}$, $\eta_{s,5}$ as a function of several factors (global solar insolation intensity, some temperatures, fluid mass flow rates, and electrical powers) [38].

Table 6
Test conditions of SAHPH mode.

Experiment time period	07.11. ÷ 10.11.2014
Experiment duration	4360 min (about 3 days)
Additional energy source	electric heater with fixed powers of 1 or 2 kW
Working fluid in the solar circuit	water
Initial water tank temperature (500 dm^3)	17.97 °C (measured by sensor $T_{3\text{-}ev,o}$)
Buffer vessel	150 dm^3 water tank
Initial water tank temperature (150 dm^3)	37.44 °C (measured by sensor Tb,i)
Total water amount in the tanks (charged by solar energy)	500 dm^3
Slope angle of the solar collectors	42°±2°
Total area of the solar collectors	6.45m^2
Position of the pyranometer	in the plane of the solar collectors
Minimal outlet fluid condenser temperature	35 °C
Maximal outlet fluid condenser temperature	43 °C
Minimal inlet fluid evaporator temperature	3 °C
Time interval of the logging measuring data	1 min
Fan coil	continuous work with air flow rate of 735 m^3/h

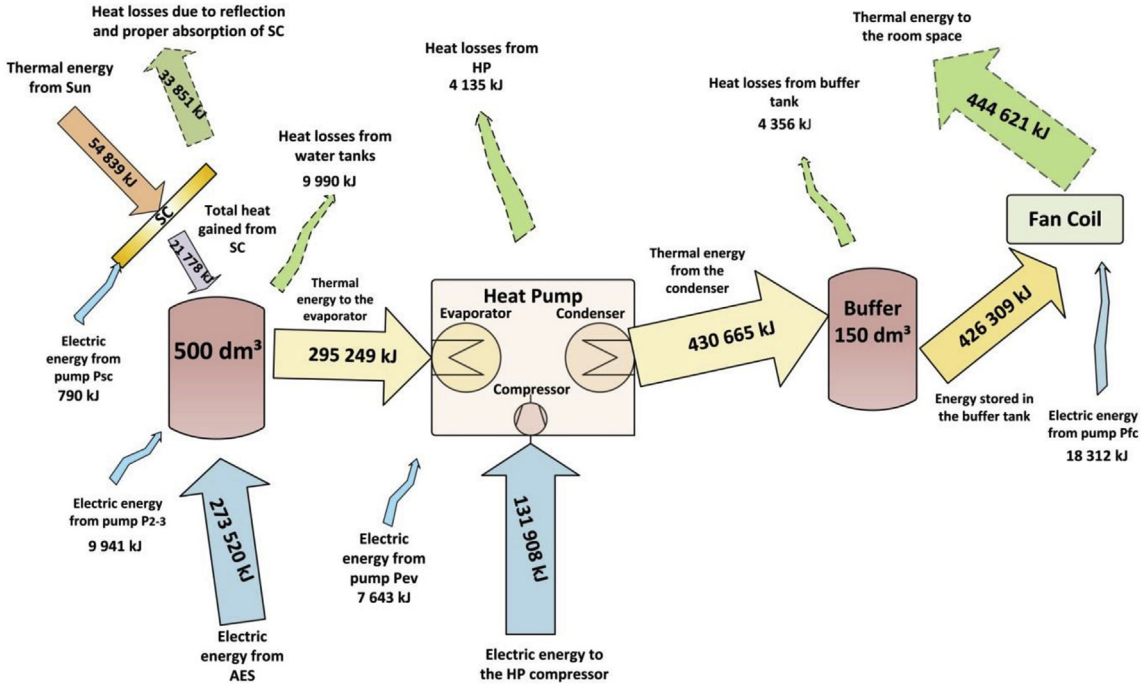

Fig. 18. Energy diagram of SAHPH mode.

The relative errors of the measured parameters are less than the accuracy presented in the Investigation methods (chapter 3.3).

The coefficient of multiple correlation R and the maximum absolute error were used as adequacy criteria of the model evaluations. The obtained values for the parameters of all the tests satisfy fully the requirements of the Investigation methods (chapter 3).

5. Conclusions

A hybrid thermal system with ground source heat pump and solar collectors was studied experimentally in five working modes. The following conclusions can be drawn:

1) The measured values of the intensity of the solar radiation falling on the SC exceeded the normal values for Plovdiv in the summer period at about 25%. This is because of the large roof panel with a height of about 4 m. Thus the roof plays the role of a nonimaging concentrator. It is recommended to use similar building roofs where the solar radiation in the plane of the collectors will be increased.
2) From the results obtained for the temperatures in the two water reservoirs (200 dm^3 and 300 dm^3) it can be concluded that the temperatures are the same. There is no stratification observed and they can be considered as one water storage tank with a volume of 0.5 m^3. It helps during the data treatment and additional storages can be situated in the same room if bigger accumulation size is needed.
3) The ground temperature increased by 1–2 °C during the charging CBTES mode (experiment duration of about 1 month). The measurements show a decrease of the ground temperature by 1.25–1.85 °C during the GSHPH mode (similar experiment duration). This proves the necessity of BHE charging with thermal energy from the sun during the summer to avoid the ground thermal depletion.

4) The system energy efficiencies of the three heating modes have been calculated - 48.59% by the DSH mode, 96.46% by the GSHPH mode and 97.95% by the SAHPH mode. The results show bigger effectiveness of the HP modes. Otherwise the SAHPH mode is applicable for short term usage because of the high needs of thermal energy from the SC (which leads to big capital investments and a need of a huge area for installation). Thus there is an obvious advantage of the GSHPH mode compared with the other two heating regimes.

Some suggestions can be made for future study with the presented installation:

1) The experiments have been done for a short period. The heating modes must be performed during longer period of time (for example one year including all the seasons). The size of the collector area should be increased - it will support the natural experiment during the SAHPH mode.
2) The installation has not been tested in GSHP cooling (GSHPC) mode and for production of domestic hot water (DHW). The GSHPC mode is a part of the heat accumulation process in the ground. Otherwise the DHW production is possible when the outlet fluid solar collector temperature is relatively high (thus the overheating will be avoided and the excess of energy will be used). The system will be studied in the mentioned operation modes.
3) The tank with a volume of 300 dm^3 was used during the experiments as a water storage. But it is constructed as a storage with a phase change material (PCM) situated in 39 steel containers. Future experiments will consider the combined work of both storages (PCM storage as a diurnal accumulator and the BTES as a seasonal storage). Other types of accumulators can be incorporated in the installation, too.
4) Data of high quality for the different system operation modes in the soil and weather conditions of the Plovdiv region have been obtained. They can be used for validation of a TRNSYS system operation model.

The presented experiments are the first step of the work which aims theoretical and experimental investigation of a hybrid heat pump system with a ground source heat pump and solar collectors. The theoretical part of the work will be published in the near future.

References

[1] W.J. Eugster, L. Rybach, Sustainable production from borehole heat exchanger systems, in: Proceedings of the World Geothermal Congress, 2000, 825–830.
[2] P. Roth, A. Georgiev, A. Busso, E. Barraza, First in-situ determination of ground and borehole thermal properties in Latin America, Renew. Energy 29 (12) (2004) 1947–1963.
[3] A. Georgiev, A. Busso, P. Roth, Shallow borehole heat exchanger: response test and charging - discharging test with solar collectors, Renew. Energy 31 (7) (2006) 971–985.
[4] S. Chapuis, M. Bernier, Seasonal storage of solar energy in borehole heat exchangers, in: 11th Int. IBPSA Conf., Glasgow, Scotland, July 27–30, 2009, 599–606.
[5] A. Chiasson, Simulation and Design of Hybrid Geothermal Heat Pumps, Ph. D. thesis, Department of Civil and Architectural Engineering, United States, University of Wyoming, 2007.
[6] Y. Man, H. Yang, Z. Fang, Study on hybrid ground-coupled heat pump systems, Energy Build. 40 (11) (2008) 2028–2036.
[7] A. Georgiev, Testing solar collectors as an energy source for a heat pump, Renew. Energy 33 (4) (2008) 832–838.
[8] C. Xi, L. Lin, Y. Hongxing, Long term operation of a solar assisted ground coupled heat pump system for space heating and domestic hot water, Energy Build. 43 (2011) 1835–1844.
[9] E. Kjellsson, G. Hellstrom, B. Perers, Optimization of systems with the combination of ground-source heat pump and solar collectors in dwellings, Energy 35 (6) (2010) 2667–2673.
[10] V. Trillat-Berdal, B. Souyri, G. Achard, Coupling of geothermal heat pumps with thermal solar collectors, Appl. Therm. Eng. 27 (2007) 1750–1755.
[11] V. Trillat-Berdal, B. Souyri, G. Fraisse, Experimental study of a ground-coupled heat pump combined with thermal solar collectors, Energy Build. 38 (12) (2006) 1477–1484.
[12] Y. Bi, G. Tingwei, Z. Liang, C. Lingen, Solar and ground source heat-pump system, Appl. Energy 78 (2004) 231–245.
[13] O. Ozgener, A. Hepbasli, Performance analysis of a solar assisted ground-source heat pump system for greenhouse heating: an experimental study, Build. Environ. 40 (8) (2005) 1040–1050.
[14] P. Cui, H.X. Yang, J.D. Spitler, Z.H. Fang, Simulation of hybrid ground-coupled heat pump with domestic hot water heating systems using HVACSIM+, Energy Build. 40 (9) (2008) 1731–1736.
[15] Huajun Wang, Chengying Qi, Enyu Wang, Jun Zhao, A case study of underground thermal storage in a solar-ground coupled heat pump system for residential buildings, Renew. Energy 34 (2009) 307–314.
[16] H.-J.G. Diersch, D. Bauer, W. Heidemann, W. Rühaak, P. P. Schätzl, Finite element modeling of borehole heat exchanger systems: Part 1. Fundamentals, Comput. Geosci. 37 (8) (2011) 1122–1135.
[17] H.-J.G. Diersch, D. Bauer, W. Heidemann, W. Rühaak, P. P. Schätzl, Finite element modeling of borehole heat exchanger systems - Part 2. Numerical simulation, Comput. Geosci. 37 (8) (2011) 1136–1147.
[18] B. Sibbitt, D. McClenahan, R. Djebbar, J. Thornton, B. Wong, J. Carrierec, J. Kokko, The performance of a high solar fraction seasonal storage district heating system – five years of operation, Energy Proc. 30 (2012) 856–865.
[19] B. Sibbitt, D. McClenahan, R. Djebbar, J. Thornton, B. Wong, J. Carriere, J. Kokko, Measured and simulated performance of a high solar fraction district heating system with seasonal storage, in: Proc. of the ISES Solar World Congress, 28 August - 2 September, Kassel, 2011.
[20] K.W. Tordrup, S.E. Poulsen, H. Bjørn, An improved method for upscaling borehole thermal energy storage using inverse finite element modelling, Renew. Energy 105 (2017) 13–21.
[21] J.S. McCartney, S. Ge, A. Reed, N. Lu, K. Smits, Soil-borehole thermal energy storage systems for district heating, in: Proc. of the European Geothermal Congress, CD-ROM, Pisa, Italy, 2013. June 3-7. 1-10.
[22] K. Bär, W. Rühaak, B. Welsch, D. Schultea, S. Homuth, I. Sass, Seasonal high temperature heat storage with medium deep borehole heat exchangers, Energy Proc. 76 (August 2015) 351–360.
[23] B. Welsch, W. Rühaak, D.O. Schulte, K. Bär, A comparative study of medium deep borehole thermal energy storage systems using numerical modelling, in: Proc. of the World Geothermal Congress 2015, 19-25 April, 2015. Melbourne, Australia, 29024.pdf.
[24] B. Welsch, W. Rühaak, D.O. Schulte, J. Formhals, K. Bär, I. Sass, Co-simulation of geothermal applications and HVAC systems, Energy Proc. 125 (September) (2017) 345–352.
[25] D.O. Schulte, W. Rühaak, B. Welsch, I. Sass, BASIMO – borehole heat exchanger array simulation and optimization tool, Energy Proc. 97 (November 2016) 210–217.
[26] B. Sibbitt, T. Onno, D. McClenahan, J. Thornton, A. Brunger, J. Kokko, B. Wong, The drake landing solar community project – early results, in: Proc. of the 32nd Annual Conference of the Solar Energy Society of Canada, Calgary, Alberta, 10-13 June 2007.
[27] B. Sibbitt, D. McClenahan Seasonal Borehole Thermal Energy Storage – Guidelines for Design & Construction, Task 45 Large Systems, IEA-SHC TECH SHEET 45.B.3.1, pp. 1-15.
[28] J. Nussbicker-Lux, H. Drück, The BTES project in Crailsheim (Germany) - monitoring results, Innostock 2012, in: 12th Int. Conf. on Thermal Energy Storage, Lleida, ES, May 16-18, 2012.
[29] E.T. Toshkov, Investigation of a Hybrid System with Ground Source Heat Pump and Solar Collectors, PhD Thesis, Technical university of Sofia, Plovdiv Branch, 2015 (in Bulgarian).
[30] T. Amanzholov, B. Akhmetov, A.G. Georgiev, A. Kaltayev, R.K. Popov, D.B. Dzhonova-Atanasova, M.S. Tungatarova, Numerical modelling as a supplementary tool for thermal response test, Bulg. Chem. Commun. 48 (Special Issue E) (2016) 109–114.
[31] H. Antonov, D. Danchev, Groundwater in Bulgaria, Tehnika, Sofia, 1980 (in Bulgarian).
[32] A.G. Georgiev, R.K. Popov, E.T. Toshkov, In-situ measurements of ground thermal properties around borehole heat exchangers in Plovdiv, Bulgaria, Bulg. Chem. Commun. 48 (Special Issue E) (2016) 19–26.
[33] A. Georgiev, S. Tabakova, R. Popov, Y. Todorov, Bulgarian variant of a mobile installation for ground thermal properties determination, in: Progress in Development and Application of Renewable Energy, first ed., National Taiwan University, 2009, 197–208. ISBN 978-986-01-8796-0.
[34] http://www.kippzonen.com/Product/11/CMP-3-Pyranometer, Kipp & Zonen products: CMP3 Pyranometer - Introduction sheet and specifications, last access - 15.10.2018.
[35] http://attachments.content4us.com/manuals/FRNED/MANUAL_EL-EPM02FHQ.PDF, Energy meter – specifications and manual, last access - 15.10.2018.

[36] ASHRAE/ANSI Standard 93–2003, Methods of Testing to Determine the Thermal Performance of Solar Collectors, American Society of Heating, Refrigeration, and Air Conditioning Engineers, Atlanta, GA, 2003.
[37] D. Pahud, Geothermal Energy and Heat Storage, Technical Report, UNSPECIFIED, 2002.
[38] E. Bozhanov, I. Vuchkov, Statistical Methods for Modelling and Optimization of Multifactor Objects, Tehnika, Sofia, 1983 (in Bulgarian).

Nomenclature

A: area, m^2
c: specific heat capacity, J/kgK
COP: coefficient of performance,-
I: intensity of solar radiation, W/m^2
m: mass, kg
$\dot{m}$: mass flow rate, kg/s
N: electrical power, W;
Q: heat, J;
$\dot{Q}$: heat flow rate, W;
R_b: borehole thermal resistance, mK/W
t: temperature, °C

Greek letters

δ: declination, °
η: efficiency
φ: geographic latitude, °
λ: thermal conductivity, W/mK
ρ: density, kg/m^3
τ: time, s; h; d.

Subscripts

2–3: 200 dm^3 to 300 dm^3 water tank
3–2: 300 dm^3 to 200 dm^3 water tank
2-sc: between 200 dm^3 water tank and solar collectors
a: ambient
ab: absorber
AES: additional energy source
BHE: borehole heat exchanger
BHE,1; BHE,10; BHE,20; BHE,30; BHE,40; BHE,50: borehole heat exchanger depth of 1, 10, 20, 30, 40 and 50 m correspondingly
b: buffer
c: condenser
end: end
ext: extracted
ev: evaporator
fc: fan coil
hp: heat pump;
i: inlet;
in: initial
inj: injected
lab: laboratory
loss: loss
o: outlet;
s: system
sc: solar collector
st: storage